Eissa *et al. Egypt J Radiol Nucl Med (2024) 55:105*
https://doi.org/10.1186/s43055-024-01275-2

Egyptian Journal of Radiology and Nuclear Medicine

RESEARCH

Open Access

Grading of skull base meningiomas by combined perfusion: arterial spin labeling and T2* dynamic susceptibility perfusion

Lamya Eissa[1*], Omneya Gamaleldin[1] and Mohamed Hossameldin Khalifa[1]

Abstract

Background Conventional MRI has no distinction between high- and low-grade meningiomas, which has a crucial for choice of therapeutic plan, especially skull base meningiomas which need more meticulous endoscopy-approached surgery. The aim of our study was to evaluate role of perfusion by arterial spin labeling and dynamic susceptibility perfusion in grading of skull base meningiomas.

Results The relative arterial spin labeling (ASL), tumor blood flow (TBF), and tumor blood volume (TBV) ratios showed significant differences between low- and high-grade meningiomas.

Conclusions MRI perfusion is a useful in differentiation between low- and high-grade meningiomas. There is significant correlation between ASL and DSC perfusion supporting possibility of using ASL in clinical practice as an alternative technique to DSC perfusion, particularly for patients with renal impairment where no contrast injection needed.

Keywords MRI, Meningioma, Perfusion

Background

Meningiomas are the most common primary benign intracranial tumor comprising nearly 16–36.1% of all intracranial tumors in adults. The "World Health Organization-WHO" classified meningiomas into fifteen histological subtypes, and into three grades based on their malignant behavior [1]. Although meningiomas are overall accounted as benign, the high-grade meningiomas (WHO grade II and III) make up nearly 20–30% of total newly diagnosed meningiomas and have been linked with high recurrence, (WHO Grade-II meningioma), exhibiting recurrence rates up to 50%, with 10-year-survival rates of less than 80% [2]. The WHO Grade III meningiomas have a recurrence rate up to 94%, with low survival rate [3]. About 30% of intracranial meningiomas are occupying skull base and labeled as skull base meningiomas (SBMs) [4].

The distinction between malignant and benign meningiomas is important before surgery because of their different recurrence rates, and to help in pre-operative planning, adjunctive radiation-therapy, and in active surveillance, especially when tumors are located at the skull base or other regions that do not easily allow surgical resection or even biopsy, and also identifying tumor-grading is a valuable prognostic aid affecting patient's morbidity and mortality [5].

Previous research attempts to predict the biological behavior or recurrence rates of meningiomas have identified variable epidemiological and radiological characters, considered to link with recurrence rate and prognosis. Gender, age, tumor size, degree of peri-tumoral edema, presence of calcifications, irregular tumor-margins, indistinct tumor–brain interface, and tumor heterogeneous enhancements, are all related to the tumoral growth speed. Still, the known imaging features of meningiomas on conventional magnetic resonance imaging-MRI have

*Correspondence:
Lamya Eissa
lamya.eissa@gmail.com
[1] Radiology Department, Alexandria Faculty of Medicine, Alexandria 21131, Egypt

no specific features that would reliably discriminate between benign and malignant tumors [6, 7].

Advanced perfusion MR-imaging can reflect characteristics of the regional blood supply, an essential biological marker of tumor-grade, and prognosis which is not available by conventional MRI-methods [5]. The two most common methods of MR-imaging used for assessing brain perfusion are: dynamic susceptibility contrast (DSC) and arterial spin labeling (ASL), with more extensive clinical application for DSC perfusion MRI [8].

The aim of the present pilot study was to determine the role of arterial spin labeling (ASL) for differentiation between low- and high-grade meningiomas by MR perfusion imaging and to compare these results with those obtained from T2 dynamic susceptibility contrast (DSC) method and from histopathology.

Methods

Patients

This pilot study aimed at patients from the "neurosurgery department," referred to the Radiology department of our "main university hospital." The protocol of this *prospective* study was approved by the "ethics committee," and an informed consent was taken from patients prior to imaging. We aimed to collect patients in duration from December 2022 to December 2023. *Inclusion criteria* included: Adult patients with CT or prior conventional images suggesting a skull base meningioma, arising from skull base bone (clivus, greater sphenoid wing, olfactory groove, jugular foramen, and cavernous sinus), either primary or recurrent case, with or without prior pathology results, while the *exclusion criteria* included (a) All claustrophobic patients, (b) patients with metallic foreign bodies, (c) patients with prior radiotherapy, radio-surgery for already known meningioma, (d) calvarium-based meningiomas are not included.

All patients underwent the following: (a) History-taking, including history of prior skull base resection, and history of renal dialysis and abnormal nodes or CBC, (b) Examination of available prior imaging of brain, (c) MRI imaging and image analysis (Detailed below), (d) Confirmation of diagnosis by biopsy and pathology.

MRI imaging

MRI images were performed on Achieva, 1.5-Tesla, Philips Medical Systems, by using a dedicated 16-channel sense neuro-vascular head-and-neck coil. (I) Conventional MRI-protocol: The protocol was tailored to cover skull base and upper neck. The standard MR brain acquisition-parameters were as follows: (a) Rapid scout images, (b) Multiplanar axial, coronal, and sagittal T2-weighted, (c) Fast spin-echo images; TR = 5000 ms, TE = 102 ms, NA-averages = 2, matrix = 256 × 256, section thickness = 5.0 mm, gap = 2.5 mm, (d) axial T1-weighted images: TR, 675 ms, TE = 8 ms, NA = averages = 2, section thickness = 5.0 mm, gap = 2.5 mm, matrix = 256 × 256.

DWI MRI

DWI was performed by using a single-shot spin echo EPI sequence, with the following parameters: Single-shot turbo-spin-echo (SS-TSE)-DWI was used): Axial 4-mm section thickness, FOV of 240 mm, and *b*-values of 0 and 1000 s/mm^2. ADC maps were generated from images by ROIs placed on the DWIs, and ADC values were calculated using the workstation software, while ROIs were placed upon solid portions of the lesion avoiding necrotic areas. Three ADC values were got, and the mean ADC was the value used in statistical analysis.

Arterial spin labeling

The pseudo-continuous ASL imaging was acquired through the use of a single-phase fast spin echo-planar imaging technique in control, and labeled images. Included parameters of ASL scanning were: Duration of labeling was = 1600–1700 ms, followed by 1200–1300 ms post-labeling delay, TR/TE = 4200–4800/13–18 ms, flip angle 35°, 3.5 mm slice thickness, with an 0.6–1 mm inter-slice gap, FOV = 20 cm × 22 cm, Sensitivity-Encoded SENSE factor of 2.5, and scanning duration of 4–5 min. *Image analysis* The ASL maps were derived from the subtraction of the labeled images from control images. Manual drawing of the region of interests (ROIs) was done by an electronic cursor and was put on ASL image encompassing the lesion. The TBFs and TBVs were calculated for tumor and normal adjacent brain parenchyma, followed by calculation of ratios.

Dynamic T2* perfusion

Following diffusion, T2 dynamic MRI sequence was obtained by injection of gadolinium gado-pentate dimeglumine, with a dose of 0.1 mmol/kg, and at a rate of 2 ml/s, using a power injector, followed by 20 ml saline flush. Sequential images were made through lesion in axial plane, and at different time intervals (at 30, 60, 90, 120, 150, 180, 240, and 300 s, following injection). Following dynamic acquisition, post-contrast MRI fat-suppressed images are obtained in axial, sagittal and coronal planes, with the same parameters, as non-contrast axial T1 images, and then subtraction is provided in axial images. The perfusion images are read on workstation by generated color maps (= Blood perfusion and blood volume), with generated curves of perfusion if needed.

Post-processing and image analysis for DCE-MRI

The color maps are generated on a dedicated software on Mac-Book Pro after drawing the ROI on the lesion, which covers the solid enhancing portion of the lesion, while vessels, necrosis, calcifications, and hemorrhages are avoided. Sufficient ROI must be obtained, at least 50% of cross-sectional area. *Image analysis* tumoral blood flow-TBF and blood volume-TBV are measured by a ROI with calculation of flow and volume ratios, as compared to normal brain parenchyma (cortex).

Statistical analysis

Statistical analyses were made with the statistical Package for Social Science version-20 (SPSS Inc., Chicago, Ill, USA). The mean and standard deviations were described for continuous data of TBF ratios, TBV ratios, and ADC values of low- and high-grade meningiomas, and are tested for statistically significant differences. The differences between TBF ratios, TBV ratios, and ADC values of low- and high-grade meningiomas were compared with the Student's *t* test. A statistically significant difference was accounted when *P* value is ≤ 0.05. Spearman correlation coefficient for TBF ratios, TBV ratios, and ADC parameters was used for inter-observer agreement assessment, and it was considered to be excellent if more than 0.80, based on calculated r-value. To ascertain a cutoff value to differentiate high- and low-grade SBMs, receiver-operating characteristic (ROC) curve for TBF ratios, TBV ratios, ADC, and combined parameters were drawn, in order to determine the area under the curve (AUC), accuracy, sensitivity, specificity, PPV, and NPV.

Results

This pilot study was conducted on 25 patients, only two males and 23 females, with ages between 20 and 70 years. The middle cranial fossa-MCF location showed highest prevalence (46% temporal fossa/sphenoid wing, and 11.5% cavernous sinus). Table 1 provides distribution of different parameters among low- and high-grade SCMs. Tumor-signal in T1 or T2 showed no significance, while enhancement was more avid in high-grade lesions. Dural tail had higher incidence in high-grade lesions (66.7% compared to 33.6%).

The mean ADC values did not show any significant difference among high- and low-grade lesions. TBF ratios tended to be lower in lower grade meningiomas, showing mean value of 1.0 (Range = 0.60–3.50), compared to malignant lesions, showing mean value of 3.0 (Range = 0.90–5.70). Same wise, TBV ratios tended to be lower in lower grade meningiomas, showing mean value of 0.90 (Range = 0.80–3.0), compared to malignant lesions, showing mean value of 4.0 (Range = 1.0–5.0). Also ASL relative was lower in low-grade lesions, showing mean value of 1.0 (Ratio = 0.70–3.0), as compared to higher values in

Table 1 Relation between final diagnoses with convention MRI parameters

Parameter	Total sample (n = 26) (%)	Final diagnosis		χ^2/p
		Low grade (n = 17) (%)	High grade (n = 9) (%)	
Site				
Anterior skull base	7.7	11.8	0.0	$^{FE}p = 0.529$
Left cavernous sinus	11.5	17.6	0.0	$^{FE}p = 0.180$
Left jugular foramen	3.8	0.0	11.1	$^{FE}p = 0.161$
Right jugular foramen	3.8	0.0	11.1	$^{FE}p = 0.161$
Left temporal fossa	46.2	35.3	66.7	$^{FE}p = 0.218$
Right temporal fossa	23.1	35.3	0.0	$^{FE}p = 0.063$
Prepontine cistern	3.8	0.0	11.1	$^{FE}p = 0.161$
Cavernous sinus	7.7	11.8	0.0	$^{FE}p = 0.529$
T1 signal				
Hypo	53.8	41.2	77.8	
ISO	46.2	58.8	22.2	$^{FE}p = 0.110$
T2 signal				
Hypo	34.6	29.4	44.4	
ISO	53.8	64.7	33.3	
Slightly hyper	7.7	0.0	22.2	$^{MC}p = 0.125$
Hyper	3.8	5.9	0.0	
Enhancement				
Low	23.1	35.3	0.0	$^{MC}p = 0.003^{*}$
Intermediate	23.1	35.3	0.0	
Avid	53.8	29.4	100	
Dural tail				
None	65.4	82.4	33.3	$^{FE}p = 0.028^{*}$
Yes	34.6	17.6	66.7	
Recurrent	42.3	64.7	0.0	
Orbital extension				
None	80.8	70.6	100.	$^{FE}p = 0.129$
Yes	19.2	29.4	0.0	
Neural foramen extension				
None	96.2	100.	88.9	$^{FE}p = 0.346$
Yes into IAC	3.8	0.0	11.1	
Susceptibility				
No	84.6	82.4	88.9	$^{FE}p = 1.000$
Blooming/peripheral	15.4	17.6	11.1	

$^{*}p < 0.001$

Table 2 Relation between final diagnoses with diffusion and perfusion parameters

	Total sample (n = 26)	Final diagnosis		U/*p*
		Low grade (n = 17)	High grade (n = 9)	
ADC	0.90 (0.70–1.20)	0.90 (0.70–1.20)	0.90 (0.70–1.20)	0.958
ASL relative	1.1 (0.70–4.0)	1.0 (0.70–3.0)	3.0 (0.80–4.0)	0.029*
BF ratio	1.15 (0.60–5.70)	1.0 (0.60–3.50)	3.0 (0.90–5.70)	0.009*
BV ratio	1.10 (0.80–5.00)	0.90 (0.80–3.0)	4.0 (1.0–5.0)	< 0.001*

Not normally distributed quantitative parameters was expressed and median (range)

U Mann–Whitney test

*Statistically significant at $p \leq 0.05$

Table 3 Multivariate analysis of various parameters

	p	OR	95% CI	
			LL	UL
ASL relative	0.084	0.0001	0.000	3.108
BF ratio	0.846	1.418	0.042	48.075
BV ratio	0.049*	6025.485	1.043	34,812,126

OR odd ratio, *LL* lower limit, *UL* upper limit, *CI* confidence interval

*Statistically significant at $p \leq 0.05$

high-grade meningiomas, showing mean ASL relative of 3.0 (Range = 0.80–4.0). Refer to Table 2 showing statistical difference. A multi-variant analysis (Table 3), however, showed no statistical significance, likely due to small sample size.

The ROC analysis for ASL relative showed a cutoff of 1.3 revealed a sensitivity of 66.7% and specificity of 94.1%, while for tumoral blood flow ratio, a cutoff of 1.6 achieved a sensitivity of 66.7% and a specificity of 94/1%, and TBV ratio of 1.5 showed a sensitivity of 77.8, and a specificity of 94.1%. These ratios revealed good NPVs and PPVs, as detailed in Table 4, and ROC analysis (Fig. 1a, b).

Linear regression analysis was performed at the current study and showed significant correlation between rCBF obtained from both DSC and ASL perfusion studies ($r2 = 0.845$; $P < 0.001$), as shown in Fig. 2a–c.

Discussion

MR perfusion imaging utilizes more developed techniques to noninvasively measure cerebral perfusion, via assessment of variable hemodynamic measures, such as cerebral blood volume (CBV), cerebral blood flow (CBF), and mean transit time (MTT). It has a great potential in labeling tumoral angiogenesis and vascular proliferation, and both are important parameters in tumor grading [5].

ASL perfusion was first reported by Deter et al. [9], who provided absolute quantification of cerebral blood flow (CBF), utilizing magnetically labeled water molecules in arterial blood, by inversion as an endogenous tracer, and without the use of contrast agents, making ASL a promising technique for analyzing perfusion in patients with renal failure and in those who require repetitive follow-ups.

DSC perfusion is based on T2-weighted imaging that measures perfusion, using an exogenous contrast agent. The nature of contrast material (exogenous gadolinium-based in DSC-MR, and endogenous tracer in ASL-MR), and different post-processing algorithms used in these two techniques, can offer different perfusion values [10]. ASL also provides absolute CBF values, which are obviously difficult with DSCs [11]. Previous comparative studies between ASL and DSC have suggested a promising linear correlation between the two techniques [12–14].

Table 4 Accuracy, sensitivity, and specificity measures

	AUC	p	95% CI	Cutoff#	Sensitivity	Specificity	PPV	NPV
ASL relative	0.765*	0.029*	0.543–0.987	> 1.3	66.7	94.1	85.7	84.2
BF ratio	0.810*	0.010*	0.628 -0.993	> 1.6	66.7	94.1	85.7	84.2
BV ratio	0.925*	< 0.001*	0.819–1.000	> 1.5	77.8	94.1	87.5	88.9

AUC area under the curve, *NPV* negative predictive value, *PPV* positive predictive value

*Statistically significant at $p \leq 0.05$

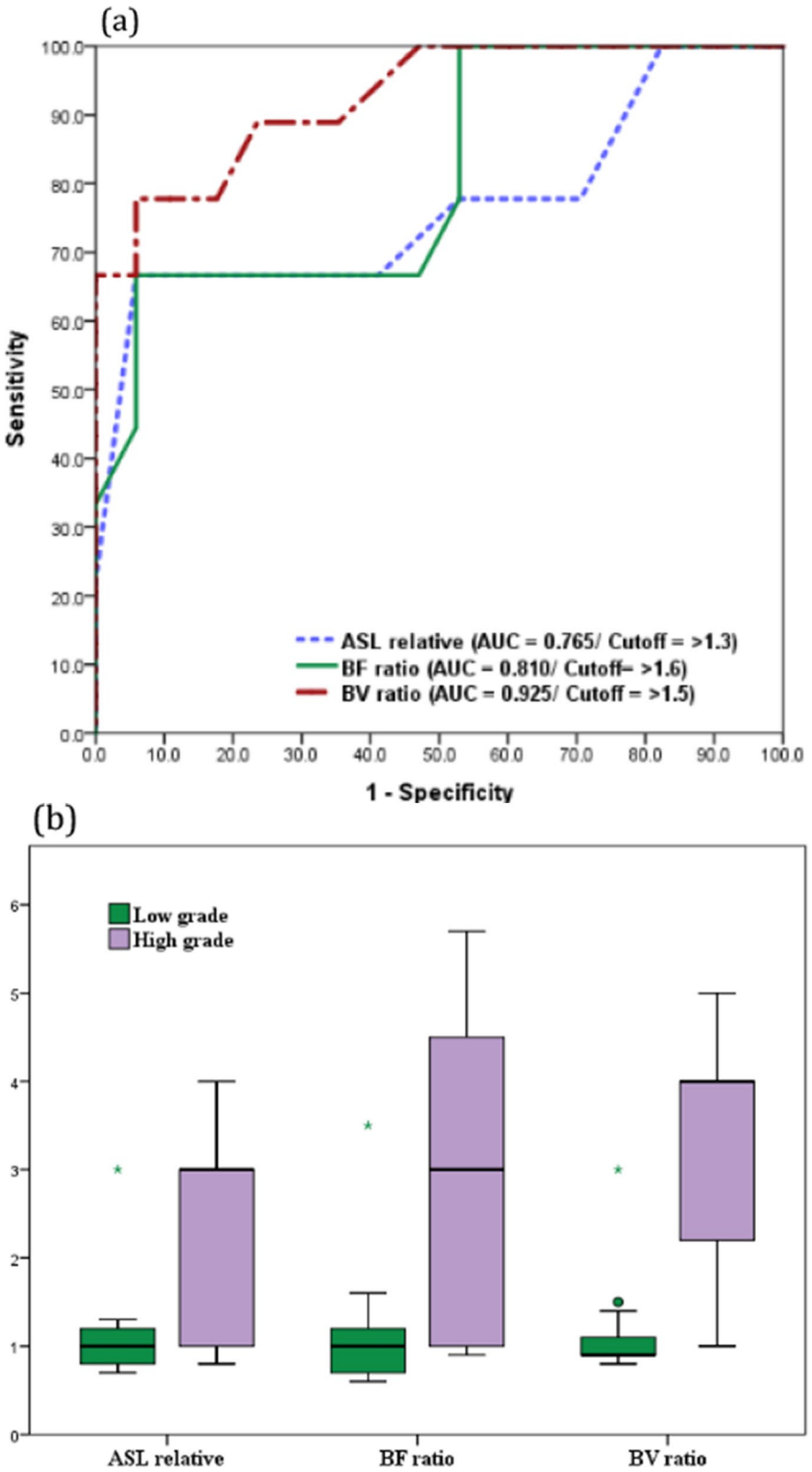

Fig. 1 The ROC for ASL relative, BF ratio, and BV ratios (**a**), (**b**)

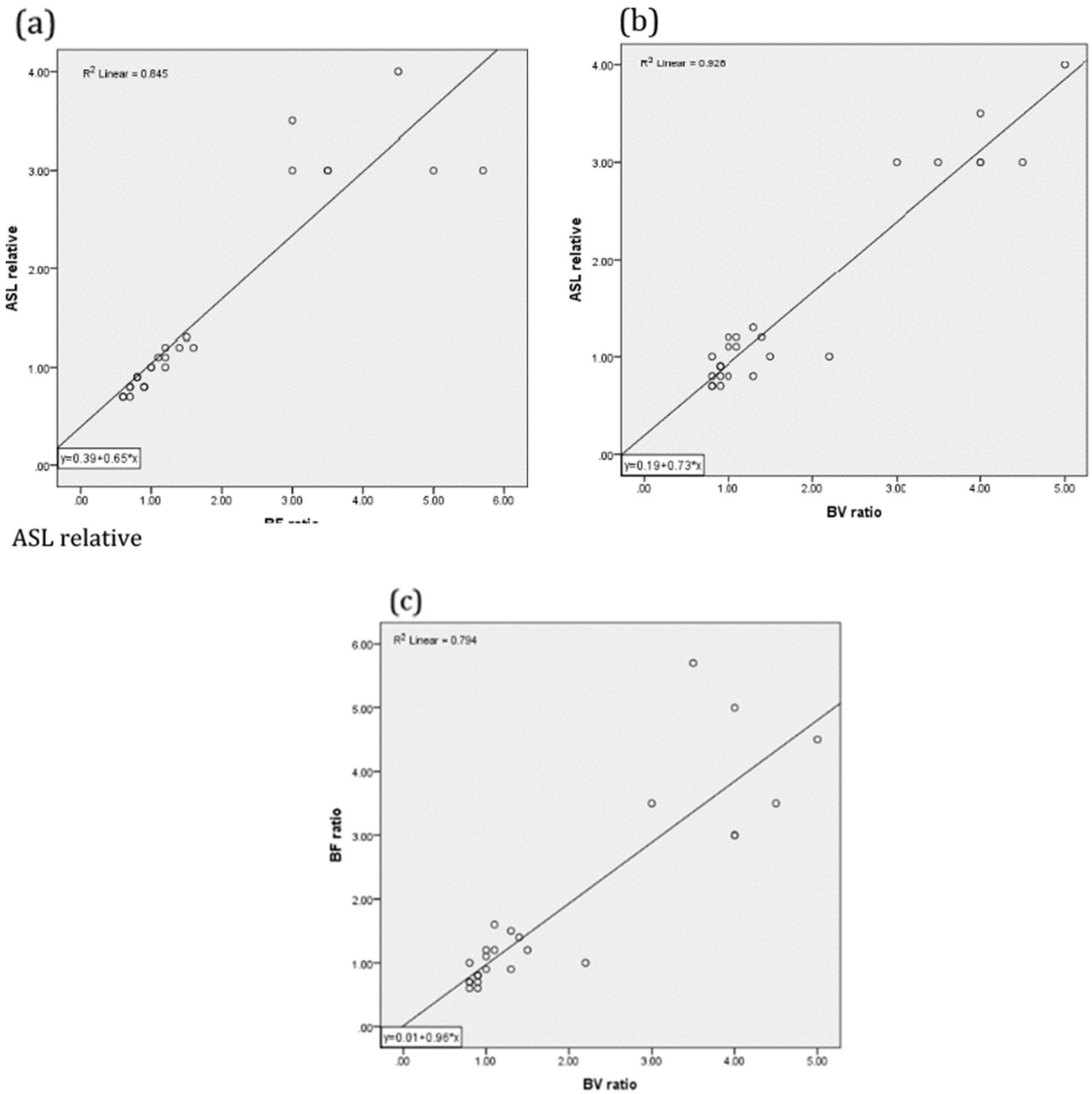

Fig. 2 The linear regression for ASL relative (**a**), TBF ratio (**b**), and TBV ratio (**c**)

Quite a few previous studies have tried to differentiate low- and high-grade meningiomas, based only on DSC perfusion (only rCBV) [15–17], or on ASL perfusion (only rCBF) [18]. In the current study, and in addition to rCBV from DSC perfusion, we have tried to assess rCBF from both ASL and DSC perfusion, in correlation with histopathological data to evaluate the role of ASL perfusion in the discrimination between low- and high-grade meningiomas and correlate it with DSC perfusion which was only previously evaluated in two studies [19, 20]—refer to Table 5, a summary of previous similar major studies in the literature.

At the current study, cases were classified into two groups, according to the final diagnosis based on histopathology or follow-up: "low-grade meningioma group" and "high-grade meningioma group." Out of 26 meningioma cases, 17 were low-grade (65.3%), while only 9 were high grade (34.7%).

The mean size of meningiomas in the current study was 4.46 cm ± 2.15 cm, compared with Magill et al.'s report of

Table 5 Summary of previous studies used perfusion MR in differentiating low- and high-grade meningiomas

	Sample size	Perfusion parameters	Main perfusion data	Statistical significance
Todua et al. [15]	29	DSC rCBV	rCBV of benign meningiomas lower than that of malignant meningiomas	($p > 0.05$)
Zikou et al. [16]	39	DSC rCBV	Grade I meningiomas had a significantly lower rCBV ratio than grade II/III meningiomas	($p = 0.031$)*
Harinath et al. [17]	30	DSC rCBV	Higher rCBV values in malignant meningiomas	($p > 0.05$)
Zhang et al. [5]	37	DSC rCBV	Higher rCBV values in low-grade meningiomas	($p > 0.05$)
Qiao et al. [18]	54	ASL rCBF	CBF of high-grade meningiomas was significantly higher than that of low-grade meningiomas	($p < 0.05$)*
Panigrahi et al. [19]	27	DSC rCBV, DSC rCBF, ASL rCBF	ASL CBF of high-grade meningiomas was significantly higher than that of low-grade meningiomas	($p < 0.05$)*
Kimura et al. [20]	21	DSC rCBV, DSC rCBF, ASL rCBF	Significant correlation between CBF values determined from both DSC and ASL perfusion methods in meningioma assessment	($p < .001$)*

*Statistically significant at $p \leq 0.05$

3.8 cm ± 1.8 cm [21]. The mean size of high-grade meningiomas (5.33 cm ± 2.33 cm) in current study was higher than that of low-grade meningiomas (4.00 cm ± 1.96 cm), but it is not statistically significant ($p = 0.148$). The difference in mean size of the current study itself in comparison with that of Magill et al. could be attributed to the timing of clinical presentation owed to different symptoms, depending on tumor location, and due to socioeconomic backgrounds. Ressel et al. [22] also reported significantly larger sizes of atypical meningiomas compared to the typical ones.

In the current study, we found statistically significant higher rCBV values in high-grade meningiomas, compared to the low-grade meningiomas (Figs. 3, 4, 5, 6), with receiver operator characteristic curve, ROC analysis yielding the highest area under the curve (AUC) of 0.925, at a cutoff value of 1.5, which could differentiate between low- and high-grade meningiomas, with a 77.8% sensitivity and a 94.1% specificity (Figs. 1, 2). Similar results had been reported by Yang et al. [23] where they reported lower rCBV values in low-grade meningiomas, with a mean of 8.02, and higher rCBV values in high-grade meningiomas, with a mean of 10.50. Our results are also supported by Todua et al. [15], who found that rCBV values in tissue parenchyma of benign meningiomas were lower than that of malignant meningiomas.

In the same context, results by Zikou et al. [16] revealed that grade I meningiomas had a significantly lower rCBV ratio than grade II/III meningiomas (median 5.1 vs. 6.4, $p = 0.031$), and they stated that using ROC curve analysis found that a rCBV ratio of 5.8 could differentiate grade I from grade II/III meningiomas, with a 82% sensitivity and a 78% specificity. Harinath et al. [17] also reported that higher rCBV values in malignant meningiomas though differences between benign and malignant meningiomas were not statistically significant ($P > 0.05$).

However, Zhang et al. [5] found completely contrasting results showing higher rCBV values in low-grade meningiomas though the difference was not statistically significant. Other studies found no correlation between rCBV and tumor grade in meningioma using a small sample size [24]. Discrepancy between the different studies could be attributed to the facts that extravasation of contrast agent following administration of gadolinium leads to T1-effects, which might corrupt the evaluation of first-pass enhancement bolus, during perfusion imaging. As extra-axial lesions are localized outside the blood–brain barrier, they are more subjected to a substantial blood pool phase [25].

Another possible explanation may be linked to differences in number of various subtypes of the typical meningiomas in different research studies. Fibroblastic meningiomas have significantly lower rCBV values than meningothelial meningiomas as found by Panigrahi et al. [19]. Thus, mean rCBV value for typical meningiomas can be affected by number of different meningiomas subtypes included in each study. Zhang et al. [5] and Kimura et al. [20] made results suggesting that among the subtypes of typical meningiomas, fibroblastic meningiomas have the lowest vascularity. On the other hand, angiomatous meningiomas have been revealed to show significantly higher tumoral relative cerebral blood volume compared with other histologic subtypes [26].

At the current study, there was statistically significant difference between low- and high-grade meningioma groups as regards rCBF ratios calculated from both DSC and ASL perfusion studies, showing higher values in the high-grade meningioma group with AUC of 0.810 for rCBF DSC and of 0.765 for rCBF ASL.

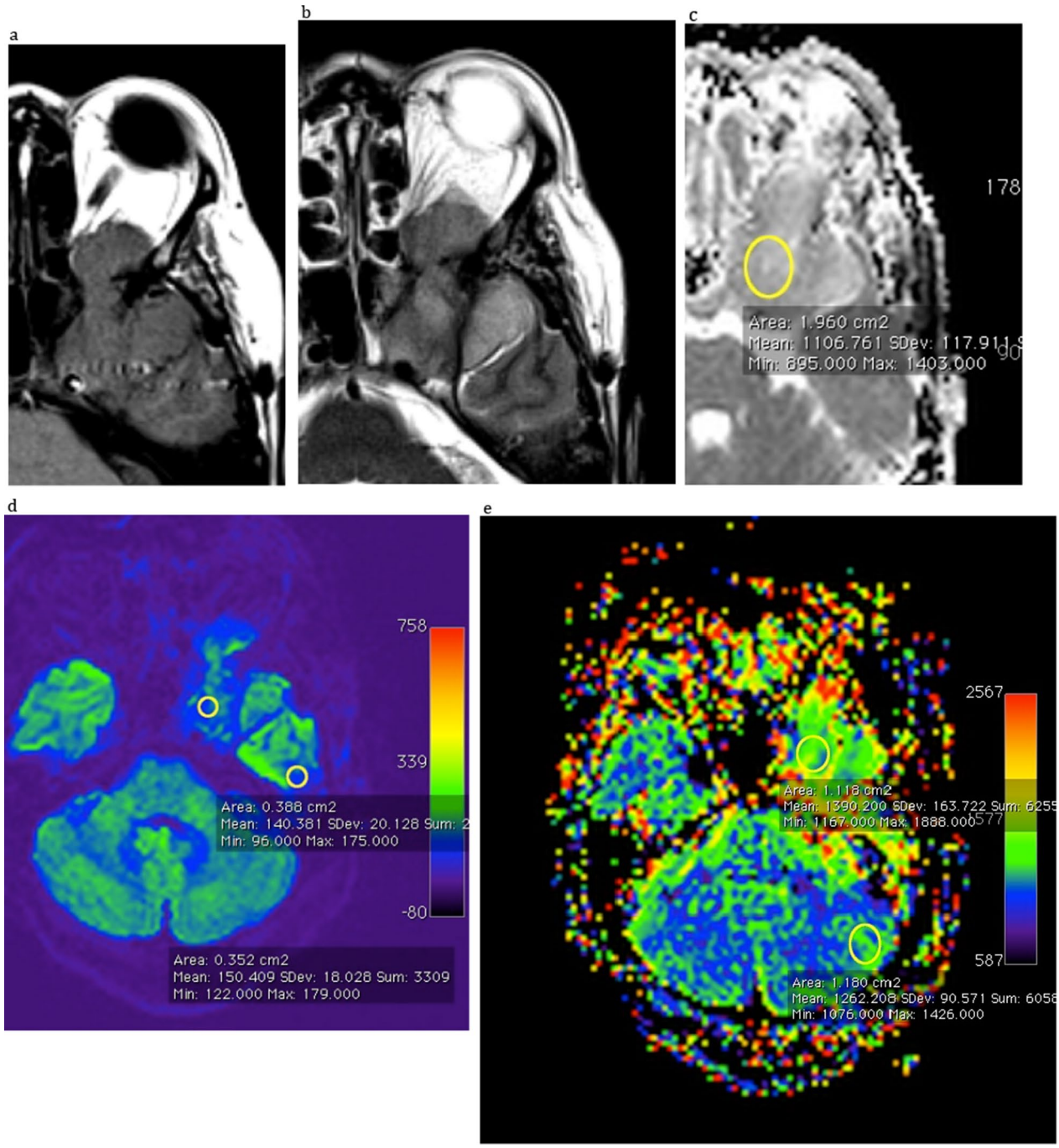

Fig. 3 Male patient 35 years old showing meningioma along sphenoid wing with orbital extension showing intermediate T1 signal (**a**), and slightly hypo-intense signal on T2 image (**b**), with an ADC value of 1.1×10^{-3} cm^2/s (**c**). Arterial spine level ASL in (**d**) showed low ASL elative (= 0.8), in contrary to higher value of TBF (= 1.1) in figure (**e**), proven later as low-grade meningioma

(See figure on next page.)

Fig. 4 A 50-year-old female with slowly growing head mass. Multiple tissues biopsied by a 20-year specialized H&N pathologist show physaliferous cells and vacuolated cytoplasm typical of Chordoma. Axial T1 (**a**) images show iso-intense signal. Axial T2 image (**b**) show heterogeneous mixed iso-hypo- and hyper-intense signals. Axial diffusion (**c**) showed ADC value of $1.2 \times 10^{-3} cm^2/s$. Contrast image (**d**) shows heterogeneous enhancement. More axial T2 images (**e**) show more hyper-intense signal. Axial ASL (**f**) image shows low ASL relative of 0.7 keeping with low-grade meningioma (*Chordoid meningioma*; *WHO-II*), as compared to higher TBF ratio of 1.2 (**g**)

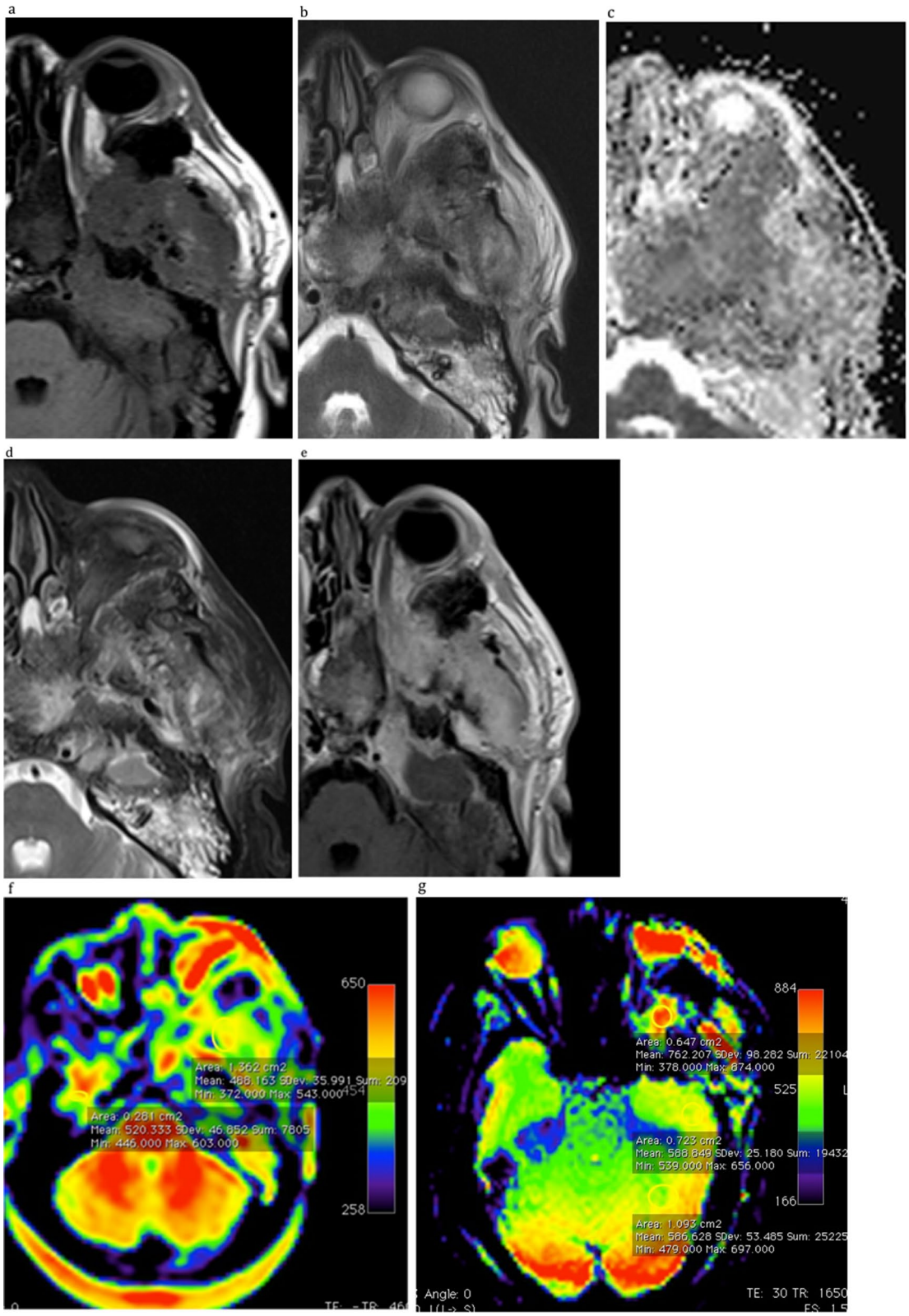

Fig. 4 (See legend on previous page.)

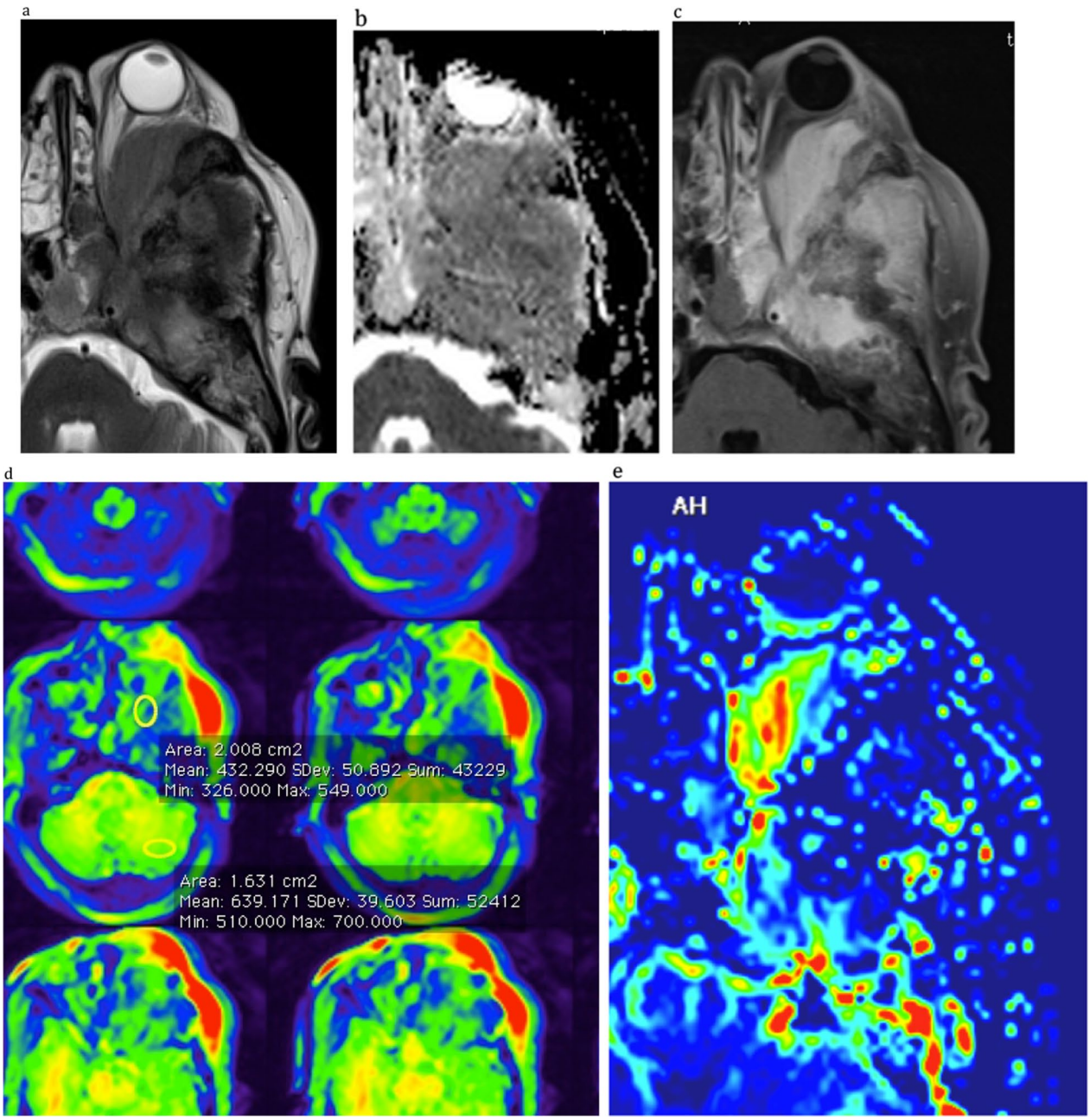

Fig. 5 A 53-year-old female is presenting with prior history of operated meningioma and recurrence of swelling, presenting also with proptosis. Axial T2 (**a**) shows sizable T2 hypo-intense mass growing from greater wing of the sphenoid bone, with trans-osseous intracranial and intra-orbital extension. Axial ADC shows value of $1.0 \times 10^{-3} cm^2/s$ (**b**), and axial T1 + contrast (**c**) shows avid homogenous enhancement. The ASL images (**d**) revealed low ASL relative (= 0.6) parallel to low TBF (= 0.7) at DSC images (**e**), both keeping with *low-grade meningioma*

In line with our study, Panigrahi et al. [19] found a significant difference between the mean CBFs of low- and high-grade meningiomas, using ASL perfusion ($p = 0.0000141$) with CBF of high-grade meningiomas significantly higher than that of low-grade meningiomas. Higher CBF in high-grade meningiomas could be attributed to their higher metabolic activity. Perfusion MR detects vascularity inside a tissue and can indirectly measure their metabolic activity, since vasculature reflects on perfusion, to fulfill metabolic demands of tissues [16]. It was also reported by other studies that CBF measurement using ASL perfusion imaging was significantly correlated with histopathological microvascular density (MVD) in meningiomas [27].

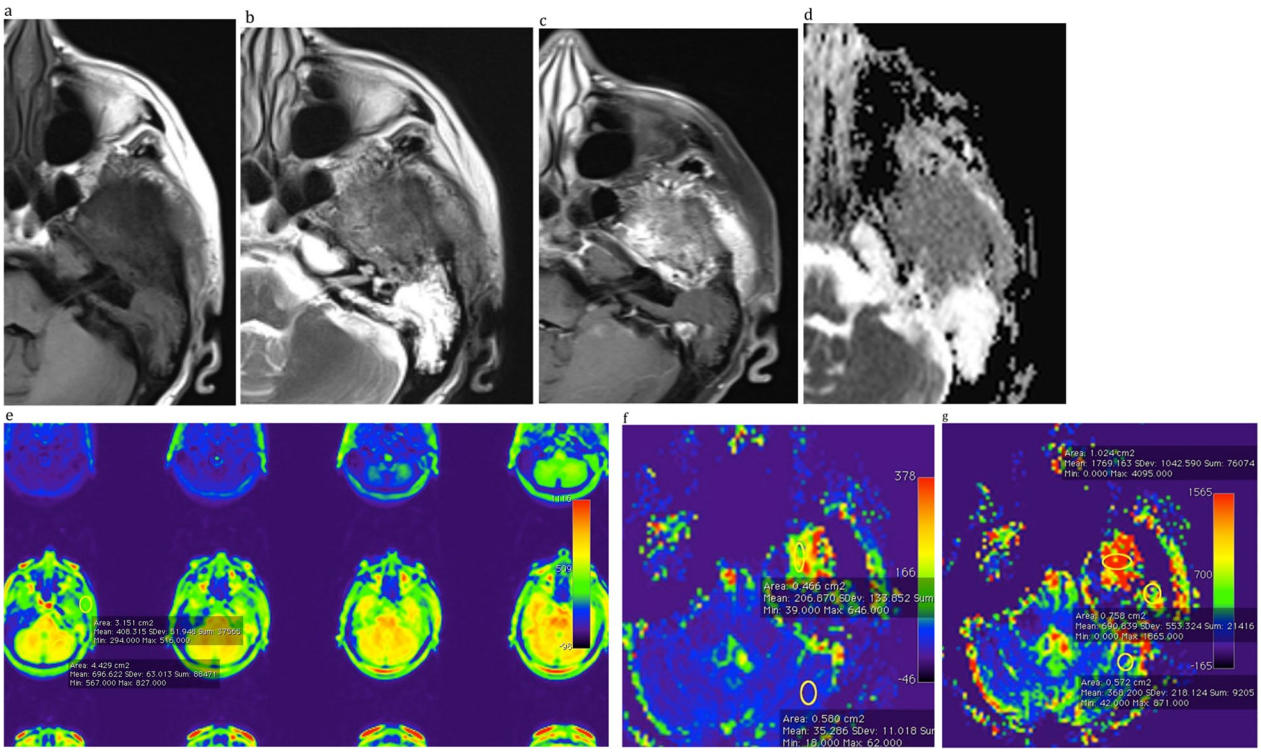

Fig. 6 A 69 years old female with severe headache, left eye proptosis and left scalp mass. **a** Axial T1shows T2 hypo-intense signal, **b** Axial T2 shows Hypo-intense signal of mass and osseous sclerosis, post GAD in (**c**) shows avid enhancement, and Diffusion-ADC (**d**) image shows a value of 1.0 x 10^{-3}cm^2/sec. ASL images (**e**) revealed low ASL-relative of 0.6 as compared to high TBF measuring 5.7 (**f**) and high TBV ratio (= 4.5) in (**g**), keeping with high-grade meningioma

On analysis of ROC curve at the current study for distinction between low- and high-grade meningiomas, the highest area under the curve (AUC) of 0.925 was for rCBV showing a sensitivity of 77.8% and a specificity of 94.1% at a cutoff point of 1.5.

Previous studies suggest that assessment of cerebral perfusion by ASL and T2DSC was comparable in normal control patients and in patients having strokes, while other studies found a good correlation between ASL and T2DSC perfusions in brain tumors [28, 29]. This is consistent with results from current study, which demonstrated comparable results in terms of meningioma CBF measurements when using either ASL or T2DSC.

Linear regression analysis was performed at current study and showed significant correlation between rCBF, obtained from both DSC and ASL perfusion studies ($r2 = 0.845$; $P < 0.001$), This is matching with results by Kimura et al. [20], who also found significant correlation between CBF values, derived from both DSC and ASL perfusion methods in meningioma assessment ($r2 = 0.73$; $P < 0.001$). The slope of correlation, however, was less than unity in regression from T2DSC-rCBF to CASL-rCBF.

Although data from the current study are encouraging, our study limitation was the small sample size, and although histopathological correlation was done to confirm meningiomas-grade, it lacked differentiation between different histological subtypes. Still controversial results from different studies on the role of perfusion for meningioma grading require further large sample studies and more dedicated studies for different histological subtypes of meningiomas which would be helpful in providing more valuable data about the perfusion behavior of each subtype.

Conclusions

In conclusion, MR perfusion is a useful noninvasive method that can potentially help in differentiation between low- and high-grade meningiomas. There is significant correlation between ASL and DSC perfusion, supporting the possibility of using ASL in clinical practice as an alternative to DSC perfusion particularly for patients with renal impairment where no contrast injection needed.

Abbreviations

DSC	Dynamic susceptibility contrast
SBM	Skull base meningioma.
MRI	Magnetic resonance imaging
ADC	Apparent diffusion coefficient

T2*	Dynamic T2-weighted imaging
CASL	Continuous arterial spin labeling
PCASL	Pseudo-continuous arterial spin labeling

Acknowledgements
Not applicable.

Author contributions
LE provided the cases and final diagnoses, with detailed description of results. MHK gave the idea, wrote the section of introduction, and provided the whole references for introduction and discussion with making of figure legends. "All authors read and approved the final manuscript." OG made the whole final supervision on conducted research and on the written consent. "*All authors have read and approved the manuscript.*"

Funding
This study had no funding from any resource.

Availability of data and materials
The datasets used and/or analyzed during the current study are available from the corresponding author on reasonable request.

Declarations

Ethics approval and consent to participate
All procedures followed were in accordance with the ethical standards of the responsible committee on human experimentation (Institutional Review Board *(IRB)"* of Alexandria General Hospital on 14 February 2022) and with the Helsinki Declaration of 1964 and later versions. Committee's reference number is unavailable (NOT applicable). No consent was obtained from the patients since it was a retrospective study.

Consent for publication
All patients included in this research gave written informed consent to publish the data contained within this study.

Competing interests
The authors declare that they have no competing interests.

Received: 20 January 2024 Accepted: 15 May 2024
Published online: 24 May 2024

References

1. Louis DN, Perry A, Wesseling P, Brat DJ, Cree IA, Figarella-Branger D et al (2021) The 2021 WHO classification of tumors of the central nervous system: a summary. Neuro-Oncology 23(8):1231–1251
2. Budohoski KP, Clerkin J, Millward CP, O'Halloran PJ, Waqar M, Looby S et al (2018) Predictors of early progression of surgically treated atypical meningiomas. Acta Neurochir (Wien) 160(9):1813–1822
3. Moliterno J, Cope WP, Vartanian ED, Reiner AS, Kellen R, Ogilvie SQ et al (2015) Survival in patients treated for anaplastic meningioma. J Neurosurg 123(1):23–30
4. Claus EB, Bondy ML, Schildkraut JM, Wiemels JL, Wrensch M, Black PM (2005) Epidemiology of intracranial meningioma. Neurosurgery 57(6):1088–1095
5. Zhang H, Rodiger LA, Shen T, Miao J, Oudkerk M (2008) Perfusion MR imaging for differentiation of benign and malignant meningiomas. Neuroradiology 50(6):525–530
6. Kawahara Y, Nakada M, Hayashi Y, Kai Y, Uchiyama N, Nakamura H et al (2012) Prediction of high-grade meningioma by preoperative MRI assessment. J Neurooncol 108(1):147–152
7. Watanabe Y, Yamasaki F, Kajiwara Y, Takayasu T, Nosaka R, Akiyama Y et al (2013) Preoperative histological grading of meningiomas using apparent diffusion coefficient at 3T MRI. Eur J Radiol 82(4):658–663
8. Soni N, Dhanota DPS, Kumar S, Jaiswal AK, Srivastava AK (2017) Perfusion MR imaging of enhancing brain tumors: comparison of arterial spin labeling technique with dynamic susceptibility contrast technique. Neurol India 65(5):1046–1052
9. Detre JA, Leigh JS, Williams DS, Koretsky AP (1992) Perfusion imaging. Magn Reson Med 23(1):37–45
10. Ata ES, Turgut M, Eraslan C, Dayanir YO (2016) Comparison between dynamic susceptibility contrast magnetic resonance imaging and arterial spin labeling techniques in distinguishing malignant from benign brain tumors. Eur J Radiol 85(9):1545–1553
11. Petersen ET, Zimine I, Ho YC, Golay X (2006) Non-invasive measurement of perfusion: a critical review of arterial spin labelling techniques. Br J Radiol 79(944):688–701
12. Lehmann P, Monet P, de Marco G, Saliou G, Perrin M, Stoquart-Elsankari S et al (2010) A comparative study of perfusion measurement in brain tumours at 3 Tesla MR: arterial spin labeling versus dynamic susceptibility contrast-enhanced MRI. Eur Neurol 64(1):21–26
13. Warmuth C, Gunther M, Zimmer C (2003) Quantification of blood flow in brain tumors: comparison of arterial spin labeling and dynamic susceptibility-weighted contrast-enhanced MR imaging. Radiology 228(2):523–532
14. Jarnum H, Steffensen EG, Knutsson L, Frund ET, Simonsen CW, Lundbye-Christensen S et al (2010) Perfusion MRI of brain tumours: a comparative study of pseudo-continuous arterial spin labelling and dynamic susceptibility contrast imaging. Neuroradiology 52(4):307–317
15. Todua F, Chedia S (2012) Differentiation between benign and malignant meningiomas using diffusion and perfusion MR imaging. Georgian Med News 206:16–22
16. Zikou A, Alexiou GA, Goussia A, Kosta P, Xydis V, Voulgaris S et al (2016) The role of diffusion tensor imaging and dynamic susceptibility perfusion MRI in the evaluation of meningioma grade and subtype. Clin Neurol Neurosurg 146:109–115
17. Harinath D, Naseeruddin V (2023) Differentiation of benign and malignant menigiomas using advanced Mri techniques. Eur J Cardiovasc Med 13(1):383–395
18. Qiao XJ, Kim HG, Wang DJJ, Salamon N, Linetsky M, Sepahdari A et al (2017) Application of arterial spin labeling perfusion MRI to differentiate benign from malignant intracranial meningiomas. Eur J Radiol 97:31–36
19. Panigrahi M, Bodhey NK, Pati SK, Hussain N, Sharma AK, Shukla AK (2022) Differentiation between various types and subtypes of intracranial meningiomas with advanced MRI. SA J Radiol 26(1):2480
20. Kimura H, Takeuchi H, Koshimoto Y, Arishima H, Uematsu H, Kawamura Y et al (2006) Perfusion imaging of meningioma by using continuous arterial spin-labeling: comparison with dynamic susceptibility-weighted contrast-enhanced MR images and histopathologic features. AJNR Am J Neuroradiol 27(1):85–93
21. Magill ST, Young JS, Chae R, Aghi MK, Theodosopoulos PV, McDermott MW (2018) Relationship between tumor location, size, and WHO grade in meningioma. Neurosurg Focus 44(4):E4
22. Ressel A, Fichte S, Brodhun M, Rosahl SK, Gerlach R (2019) WHO grade of intracranial meningiomas differs with respect to patient's age, location, tumor size and peritumoral edema. J Neurooncol 145(2):277–286
23. Yang S, Law M, Zagzag D, Wu HH, Cha S, Golfinos JG et al (2003) Dynamic contrast-enhanced perfusion MR imaging measurements of endothelial permeability: differentiation between atypical and typical meningiomas. AJNR Am J Neuroradiol 24(8):1554–1559
24. Zhu F, Zhou Y, Wang C, Gao J, Qi J (2002) Perfusion MRI evaluation of correlating perfusion constants with histologic findings in meningiomas. In: Proceedings of the annual meeting of the international society for magnetic resonance in medicine; Berkeley, CA
25. Lui YW, Malhotra A, Farinhas JM, Dasari SB, Weidenheim K, Freeman K et al (2011) Dynamic perfusion MRI characteristics of dural metastases and meningiomas: a pilot study characterizing the first-pass wash-in phase beyond relative cerebral blood volume. AJR Am J Roentgenol 196(4):886–890
26. Zhang H, Rodiger LA, Shen T, Miao J, Oudkerk M (2008) Preoperative subtyping of meningiomas by perfusion MR imaging. Neuroradiology 50(10):835–840
27. Koizumi S, Sakai N, Kawaji H, Takehara Y, Yamashita S, Sakahara H et al (2015) Pseudo-continuous arterial spin labeling reflects vascular

density and differentiates angiomatous meningiomas from non-angiomatous meningiomas. J Neurooncol 121(3):549–556
28. Lia TQ, Guang Chen Z, Ostergaard L, Hindmarsh T, Moseley ME (2000) Quantification of cerebral blood flow by bolus tracking and artery spin tagging methods. Magn Reson Imaging 18(5):503–512
29. Hunsche S, Sauner D, Schreiber WG, Oelkers P, Stoeter P (2002) FAIR and dynamic susceptibility contrast-enhanced perfusion imaging in healthy subjects and stroke patients. J Magn Reson Imaging 16(2):137–146

Publisher's Note